Available online at www.sciencedirect.com

ScienceDirect

Energy Procedia 157 (2019) 75–83

Energy Procedia

www.elsevier.com/locate/procedia

Technologies and Materials for Renewable Energy, Environment and Sustainability, TMREES18, 19–21 September 2018, Athens, Greece

Threshold Current Density of $Al_{0.1}Ga_{0.9}N/GaN$ Triple Quantum Well Laser

Kzal Mohammed Qader, Ebtisam M-T. Salman *

Department of physics, College of education for pure science-Ibn Al-Haitham, University of Baghdad,Baghdad, Iraq

Abstract

Semiconductor laser is used in processing many issues related to the scientific, military, medical, industrial and agricultural fields due to its unique properties such as coherence and high strength where GaN-based components are the most efficient in this field. Current technological developments mention to the strong connection of GaN with sustainable electronic and optoelectronic devices which have high-efficiency. The threshold current density of $Al_{0.1}Ga_{0.9}N/GaN$ triple quantum well laser structure was investigated to determine best values of the parameters affecting the threshold current density that are well width, average thickness of active region, cavity length, reflectivity of cavity mirrors and optical confinement factor. The optimum value of the threshold current density is 2670 A/cm^2 was obtained when the well width (w= 2.5 nm), reflectivity of cavity mirrors (R1=0.75, R2=0.9), cavity length (L=2mm), average thickness of active region (d= 11.5 nm), and optical confinement factor (Γ= 0.034) at room temperature.

© 2019 The Authors. Published by Elsevier Ltd.
This is an open access article under the CC BY-NC-ND license (https://creativecommons.org/licenses/by-nc-nd/4.0/)
Selection and peer-review under responsibility of the scientific committee of Technologies and Materials for Renewable Energy, Environment and Sustainability, TMREES18.

Keywords: threshold current density, GaN, AlGaN, multiple quantum well lasers

* Corresponding author. Tel.: +0-000-000-0000 ; fax: +0-000-000-0000 .
E-mail address: emtaki66@yahoo.com

1876-6102 © 2019 The Authors. Published by Elsevier Ltd.
This is an open access article under the CC BY-NC-ND license (https://creativecommons.org/licenses/by-nc-nd/4.0/)
Selection and peer-review under responsibility of the scientific committee of Technologies and Materials for Renewable Energy, Environment and Sustainability, TMREES18.
10.1016/j.egypro.2018.11.166

1. Introduction

Semiconductor laser (SLs) technology is one of the most advanced technologies that have intensive development since the invention of laser in fifties of last century to the present and the literature on this topic is really immense. Most semiconductor lasers are based on compounds of the III-V [1,2]. The advance in III-V nitride technology leading to the availability diodes is of blue laser diodes as a recent example [3]. In fact, in the past few decades, various forms of laser have gained much attention to the treatment of more issues and their widespread use in various areas of life, especially those related to the scientific, military, medical, industrial and agricultural fields. This is due to its unique properties such as coherence and high strength [1-4]. GaN-based components are the most efficient in this field. These devices used instead of conventional lighting for domestic lighting and the roadside due to their high reliability and their little energy consumption. In addition the "nitrides and their alloys" which have basic properties of the development of ultraviolet and blue lasers, the production of systems allows the operation of digital information and greater storage capacity [5]. GaN is a promising semiconductor due to its exceptional physical properties, good mechanical properties and high chemical stability [6]. On the other hand, the emphasis continues to the present day the developments in all the III-V nitride such as GaN thin film materials, direct energy band gap. The most important feature of these materials is the proportions control of the semiconductor material components through which the light emitted wavelength can be determined. These wavelength of light emitted is often located in the visible and infrared spectra and extends to the deep ultraviolet. At present, maximizing the benefit and evaluate of the sustainable light sources dependence two important criteria energy-savings and environmental-friendliness, this is much available in LEDs[7].

The p-n junction of semiconductor materials is an base in producing semiconductor laser [1,5]. Nanostructures is a convenient and advance route for the development of semiconductor materials with new profiles, able to yield materials with property profiles superior to those of the bulk materials (large size) [8,9] such as quantum well laser. This method is usually more efficient to create laser materials with new properties than the development of new materials. During the few past decades, the production of semiconductor nanomaterials has gained considerable interest in a development of innovative materials with suitable properties to deal with challenges related of laser production. A quantum well is a special type of heterojunction in which one thin well layer is surrounded by two barrier layers. The active region of the quantum well laser structure is a narrow layer a quantum confinement occurs, according to quantum mechanics [4,10]. Quantum well laser is classified into two types single and multiple quantum well lasers. The most common structure of GaN crystal is the wurtzite structure and it is the most stable structure in thermodynamics steady state at room temperature and 1 atm. Therefore most of the GaN devices or researches are founded on the wurtzite GaN. Through its crystalline structure, the properties of GaN are determined directly [4,6]. AlGaN is the ternary alloys of wurtzite and zinc blened poly types of GaN with AlN of a continuous alloy system with a wide range of band gap and a minor change in the lattice constant. It is frequently used as the barrier material for nitride electronic and optoelectronic devices [11].

In order to achieve as good as it is possible to be performance that achieves the desired results we apply the most effective way, by choosing a structure three-quantum wells with barrier width 2 nm of III-V compounds, for further details, refer to the Ref. [12,13]. In this research, the perform optimal values of parameters of the $Al_{0.1}GaN_{0.9}$ / GaN triple quantum well laser which has been emitted wavelength 352 nm in ultraviolet radiation range are determined by well width, cavity length, average thickness of active region, reflectivity of cavity mirrors, and optical confinement factor, which performing gives by lowest threshold current density.

2. Theoretical model

The carrier recombination is the reverse process for generation process. The generation defined as the movement of an electron from the valence band to the conduction band. This leads to the creation of the electron hole pair. Recombination is that the process in which the electrons from conduction band return to valence band, which emit the energy in form light or photons. The lifetime of the minority carrier controls the rate of recombination. Recombination process is classified into two type radiative recombination and non radiative recombination [14].

The radiative recombination occurs when electron in the conduction band (CB) recombines with hole in the valence band (VB) emitting a photon. The radiative recombination rate due to spontaneous emission can be expressed by the following equation [15].

$$R_r = B_{rad}N^2 \quad (1)$$

Where *N* is the carrier concentration, B_{rad} is the radiative recombination coefficient, can be written as [16].

$$B_{rad} = \frac{e^2\, w\, n_r\, E_g\, |M_{ave}|^2}{\varepsilon_o\, C^3 m_o^2\, k_b\, T\, m_h^*(1+r)} \quad (2)$$

Where e is the electron charge, w is the well width, E_g is the energy band gap, ε_o is the permittivity in vacuum, *C* is the light velocity, m_o is the free electron mass, k_b is the Boltzmann constant, $r = \frac{m_e^*}{m_h^*}$, m_e^* and m_h^* are the electron and hole effective masses, n_r is the refractive index, $|M_{ave}|^2$ is the average of the squared of the momentum matrix element can be written as [17, 18].

$$|M_{ave}|^2 = \frac{(2M_{TE}+M_{TM})}{3} \quad (3)$$

Where M_{TE} is an average of the squared momentum matrix element for the *TE* mode can be written as [19].

$$M_{TE} = \langle M\rangle_{hh,TE} + \langle M\rangle_{lh,TE} \quad (4)$$

Where $\langle M\rangle_{hh,TE}$ and $\langle M\rangle_{lh,TE}$ are the squared momentum matrix element of the electron - heavy hole and electron - light hole interactions respectively for the *TE* mode as the following [20].

$$\langle M\rangle_{hh,TE} = \frac{3M^2}{2} \quad (5)$$

$$\langle M\rangle_{lh,TE} = \frac{M^2}{2} \quad (6)$$

And M_{TM} is an average of the squared momentum matrix element for the *TM* mode can be written as [19].

$$M_{TM} = \langle M\rangle_{hh,TM} + \langle M\rangle_{lh,TM} \quad (7)$$

Where $\langle M\rangle_{hh,TM}$ and $\langle M\rangle_{lh,TM}$ are the squared momentum matrix element of the electron - heavy hole and electron - light hole interactions respectively for the *TM* mode as the following [20].

$$\langle M\rangle_{hh,TM} = 0 \quad (8)$$

$$\langle M\rangle_{lh,TM} = 2M^2 \quad (9)$$

Where *M* is the momentum matrix element can be written by the following express [20].

$$M = \frac{m_o}{\sqrt{3}}\left(\frac{E_g(E_g+\Delta_o\ )}{2m_e^*(E_g+\frac{2}{3}\Delta_o)}\right)^{\frac{1}{2}} \quad (10)$$

Where is Δ_o is the split off energy.

Non radiative recombination happens when the carriers in the (CB) and (VB) recombine non- radiatively, this means that will not light emit from this process. This will increases the current need achieve lasing [21]. Non radiative recombination process includes defects recombination, Auger recombination and leakage current recombination. The Auger recombination coefficient can be written as [15].

$$C_{Aug} = \frac{1}{\tau_A N^2} = C_o \, exp\left(\frac{-E_a}{k_b T}\right) \quad (11)$$

Where τ_A is the Auger carrier lifetime. E_a and C_o are the activation energy and coefficient in the conduction-hole conduction-conduction (CHCC) Auger process can be written [16].

$$E_a = \frac{m_e E_g}{m_e^* + m_{hh}} \quad (12)$$

$$C_o = \frac{4\pi e^4 m_e (m_{hh} + m_e^*)|M_{ee}|^2}{\hbar \varepsilon^2 (2m_{hh} + m_e^*)^2 k_B T} \quad (13)$$

Where m_{hh} the heavy hole mass, ε is the dielectric constant, $|M_{ee}|^2$is the matrix element of the electron-electron interaction is given by

$$|M_{ee}|^2 = \left(\frac{\hbar^2}{2m_o}\right)^2 \frac{m_o E_p}{3\, m_e^* E_g^3} \quad (14)$$

Where E_p is the energy equivalent of the momentum matrix element.

The threshold current density (J_{th}) is the most common of the laser diodes. It is a direct indicator in determining the quality of semiconductor materials that are fabricated device. The threshold current density is given by [22].

$$J_{th} = ed(A_D N_{th} + B_{rad} N_{th}^2 + C_{Aug} N_{th}^3) \quad (15)$$

Where d is the average thickness of active region, A_D is the monomolecular recombination coefficient, N_{th} is the threshold carrier density can be expressed as [23].

$$N_{th} = N_{tr} exp\left(\frac{\alpha_i + \alpha_m}{\Gamma^{MQW} g_o}\right) \quad (16)$$

Where g_o is the gain coefficient, α_i is the internal loss and $\alpha_m$is the mirror loss, Γ^{MQW} is the optical confinement factor for multiple quantum well, N_{tr} is the transparency carrier density can be written

$$N_{tr} = \left[2\left(\frac{k_b T}{2\,\hbar^2}\right)^{\frac{3}{2}} (m_e^* m_h^*)^{\frac{3}{4}}\right] \quad (17)$$

3. Results and discussion

Figure (1) shown that the threshold current density (J_{th}) versus the well width (w) for different cavity length L = (0.5, 0.75, 1, 2, 3, 4) mm, can be calculated by using eqs. (11), (10) and (3), (2) and (15). It is clear that the J_{th} decreases with increasing well width for each the cavity length values where the best value is $J_{th} = 2670$ A/cm^2 which it the same value at L=2mm, L=3mm, and L=4mm, when w=2.5nm and T=300K. After this value of J_{th}, it increases with increasing w.

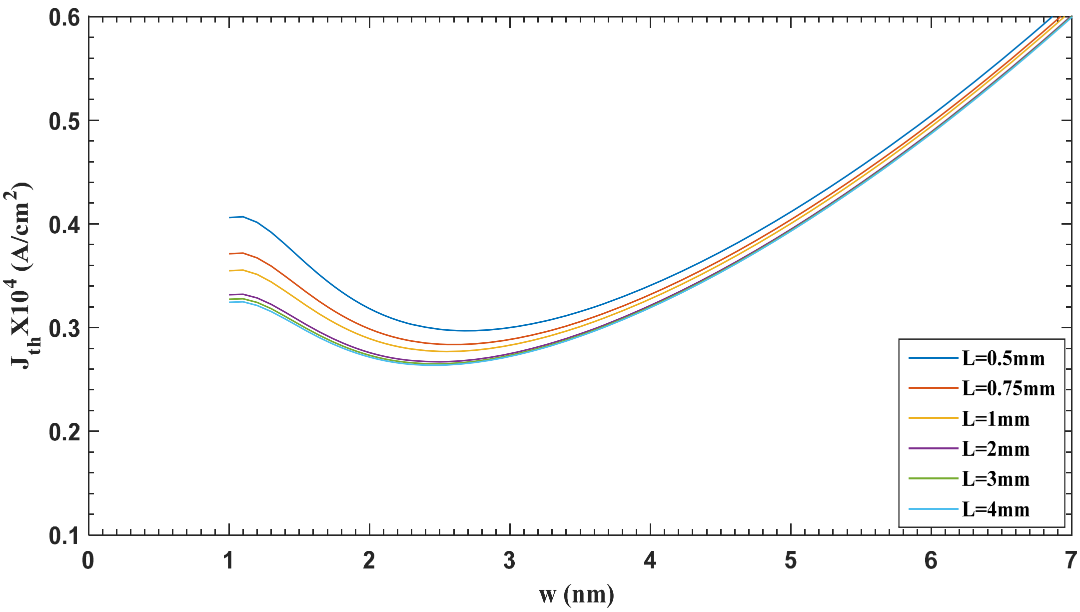

Fig. 1. The threshold current density for different cavity length versus the well width.

Equation (15) shows relation between the total threshold current density with well width (w) for several temperature T= (77,150, 200, 250, 300) K, as shown in figure (2) which was drawn by eqs (2), (3), (10) and (15). The lowest value of the threshold current density at T=77K is J_{th}= 188A/cm^2 but at T=300K is J_{th}= 2670 A/cm^2 when w=2.5 nm.

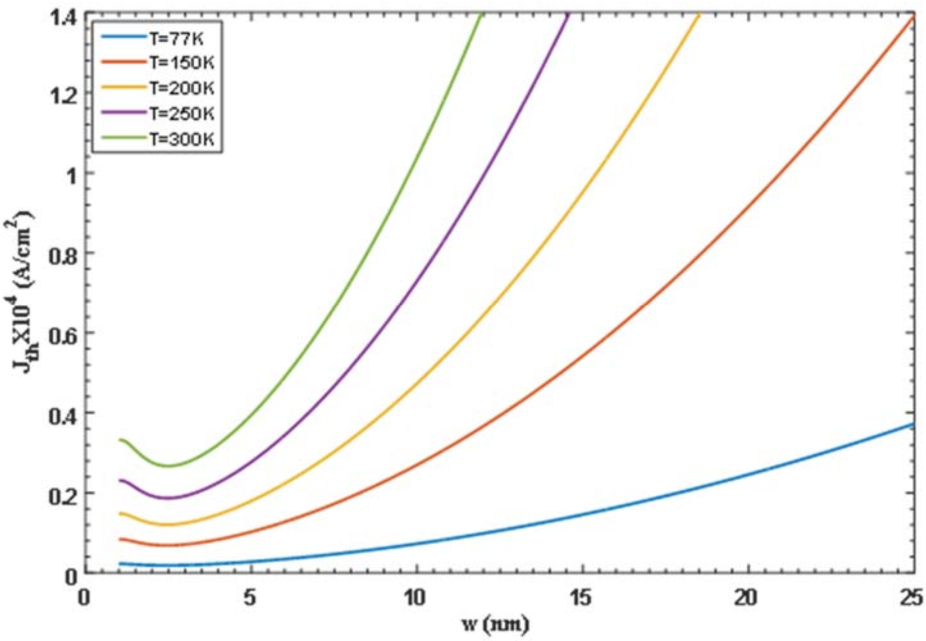

Fig. 2. The threshold current density for the different temperatures versus well width.

The threshold current density versus the average thickness of active region (d) for different temperatures (77, 150, 200, 250, 300)] K, can be calculated by using eq. (15) as shown in figure (3). It is clear that the J_{th} decreases with increase average thickness of active region for each temperature value until the arrival threshold current density to the lowest value is $J_{th} = 2670$ A/cm^2 at d = 11.5 nm , T=300K, then start increases. The 11.5 nm value of average thickness of active region is considered as the best value to reduce threshold current value and to provide more possible performance content using this simulation.

The simulation results indicate that, these effects occur because as the losses increases, the current density required as threshold increases. Hypothetically, increment of loss increases the threshold current and reduces content of structure performance. When the loss is decreased, the threshold current improved owing to the decreased the number of carriers that cross the active region without recombining effects. Thus, decreasing the loss value provides higher performance content for the laser structure. As a result, in this article, the lowest threshold current value with a lower loss is considered as the best value. Whenever, the barrier is larger, lower thermionic emission of the charge carriers outside the active region. These carriers collect in active region, leading to quasi-Fermi levels moving to more ranges. Thus, Charge carriers with energies close to quasi-Fermi levels will have lower barrier to cross without recombination or growing the gain. Increasing the confinement of charge carrier in the active region through the larger barriers and the smaller well leads to increase in the active region and thus the threshold current is lower and has a lower rate of increase with losses.

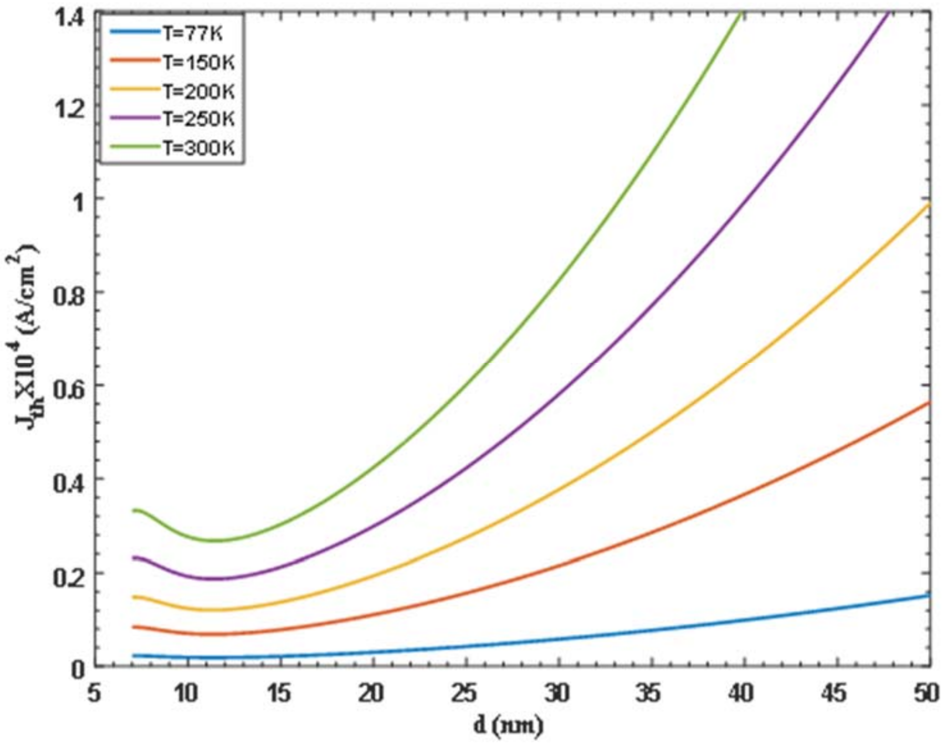

Fig. 3. The threshold current density for the different temperatures versus average thickness of active region.

The threshold current density (J_{th}) versus the cavity length (L) for different values of temperature T= (70, 150, 200, 250, 300) is shown in figure (4), using equation (15).

It's clear that the J_{th} decreases with increases cavity length for each temperature values. Next, the threshold current density for all values of cavity length that takes values greater or equal to 1 mm is almost stable; owing to the mirror loss component is proportional to the total loss with L^{-1}. An important consequence of this difference indicates that the cavity loss is not so high as to overwhelm the mirror loss. This is the determining factor in a dependence on the cavity length. Otherwise, the threshold current density does not depend on the cavity length. When the loss of the mirror is almost known, the cavity loss can be approximated from the threshold current density measurements by supposing that the optical gain is plainly proportionate to the injection current. Optimal value of threshold current density has a 2670 A/cm^2, corresponding to a cavity length is 2 mm at room temperature.

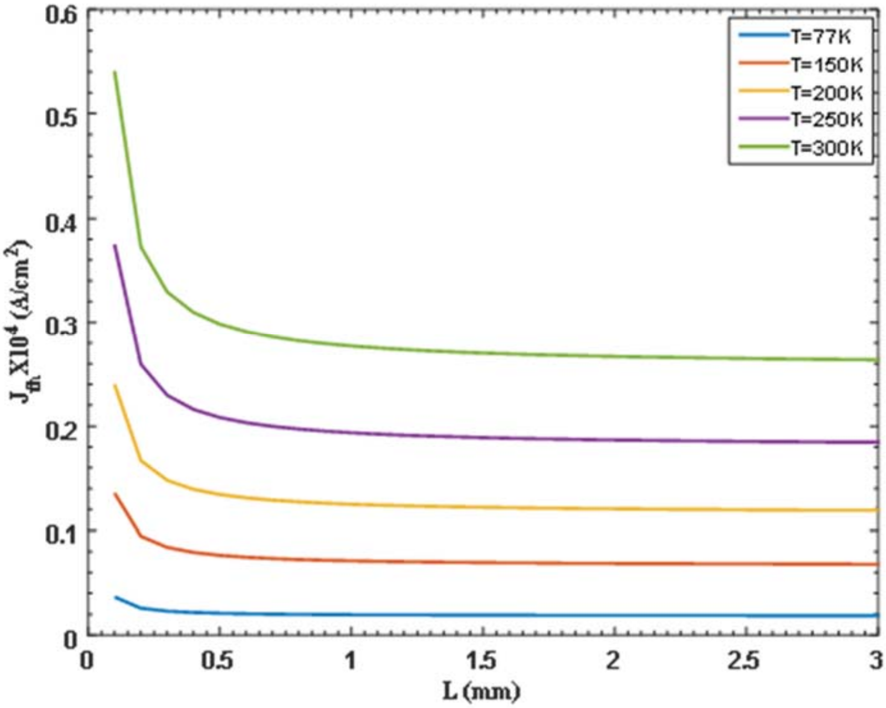

Fig. 4. The threshold current density versus cavity length for the different temperatures.

Through the previous figures for threshold current density illustrate that both J_{th} increase with increasing temperature this is the increases cavity losses with increasing temperature. To overcome cavity losses we need more current to achieve the population inversion.

The threshold current density versus the well width (w) for variations mirrors reflectivity (R1, R2) was calculated by using eq. (15) at room temperature, as shown in figure (5). This figure appears that the $J_{th} = 2670$ A/cm^2 when R1=0.75 and R2=0.9, as well as $J_{th} = 3432$ A/cm^2 when [21]

$$R1=R2=\frac{(n_r-n_{air})^2}{(n_r+n_{air})^2} \qquad (18)$$

the threshold current density value is $J_{th} = 3026$ A/cm^2 when R1=$\frac{(n_r-n_{air})^2}{(n_r+n_{air})^2}$ and R2=0.9.Through these values, it is clear that the best value of threshold current density is 2670 A/cm^2 in the case reflectivity R1=0.75 and R2=0.9.

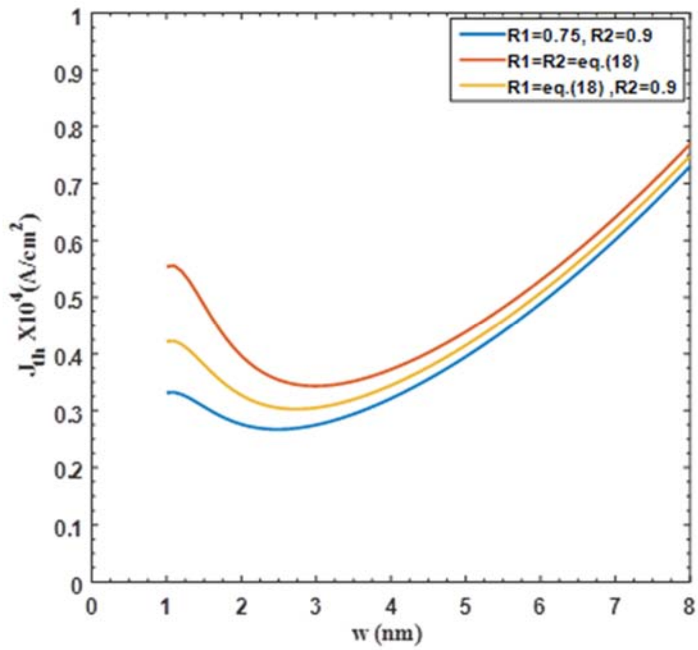

Fig. 5. The threshold current density for different reflectivity versus well width.

The threshold current density versus the optical confinement factor was calculated by using equation (15) as shown in figure (6), it shows that the best value of threshold current density is $J_{th} = 2670$ A/cm^2 at Γ= 0.034 and T=300K.

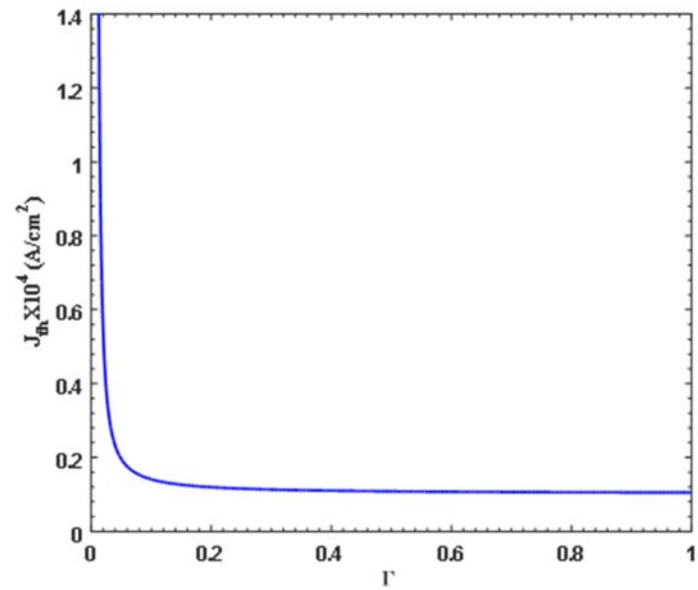

Fig. 6. The threshold current density versus the optical confinement factor.

4. Conclusions

In this study we have shown optimal values for some parameters of $Al_{0.1}Ga_{0.9}N/GaN$ triple quantum well laser structure at room temperature. Determine the optimal values of the necessary parameters which allowed the determination of the less value for threshold current density of this structure performance. It turned out that threshold current density decreases with increases cavity length for each temperature values and then begin to be constant near cavity length is equal 1mm. Accordingly, the less value of threshold current density is 2670 A/cm^2 at cavity length (2mm), when well width (2.5 nm) at room temperature. Also show that the threshold current density decreases with increase average thickness of active region for each temperature value. Where the lowest value of threshold current density is get at average thickness of active region (11.5 nm) at room temperature. In addition, that the optimal value of threshold current density (2670 A/cm^2) is in the case reflectivity of cavity mirrors for R1 and R2 are 0.75 and 0.9 respectively and optical confinement factor (0.034) at room temperature.

5. References

[1] C. Liu, Y. Li and Y. Zeng, "Progress in Antimonide Based III-V Compound Semiconductors and Devices", *Engineeing* 2(8) (2010): 617-624.

[2] S. Beg, S. H. Saeed and M. J. Siddiqui, "III-V Compound Semiconductor Laser Heterostructures Parametric Performance Evaluation For InGaAs/GaAs And AlGaAs/GaAs", *Advances in Computational Sciences and Technology* 10(10) (2017): 2985-3013.

[3] M. T. Hardy, D. F. Feezell, S. P. DenBaars and S. Nakamura, "Group III-nitride laser a materials perspective", *Materials Today* 14(9) (2011): 408-415.

[4] E. M-T. Salman, "Optical Confinement Factor of $Al_{0.7}Ga_{0.3}As/GaAs$ and $Al_{0.7}Ga_{0.3}N/GaN$ Quantum Wire Lasers", *International Journal of Science and Research* 7(1) (2018): 1304-1310.

[5] D. S. patil, *Semiconductor Laser Diode Technology and Application*, InTech, (2012).

[6] Q. Wang, *Development of enhancement-mode GaN MOSFET on AlGaN/GaN heterostructur*e, Tokushima University, (2015).

[7] I. Lo, "Advances in GaN Crystals and Their Applications", 8 (2018): 117.

[8] M. R. Jubayr, E. M-T. Salman, A. S. Kiteb, "A theoretical investigation of enhanced thermoelectric figure of merit of Low-Dimensional Structures", *Ibn Al- Haitham J. For Pure & Appl. Sci*. 23(3) (2010): 95-105.

[9] M. R. Jubayr, "The heat exchange intensification in nano-homojunction semiconductor materials", *Engineering and Technology Journal* 33(5), Part (B) Scientific (2015): 819-829.

[10] D. A. Anghel, A. R. sterian and P. E. sterian, "Modeling Quantum Well Lasers", *Mathematical Problems in Engineering* (2012): 11.

[11] Vurgaftman, J. R. Meyer and L. R. Ram-Mohan, "Band Parameters for III-V Compound Semiconductor and Their Alloys", *Journal of applied physics* 89(11) (2001): 5815-5875.

[12] J-R. Chen, T-S. Ko, P-Y. Su, T-C. Lu, H-C. Kuo, Y-K. Kuo, and S-C. Wang, "Numerical Study on Optimization of Active Layer Structures for GaN/AlGaN Multiple-Quantum-Well Laser Diodes", *Journal of Lightwave Technology* 26(17) (2008): 3155-3165.

[13] W. K. Abad, *Theoretical comparison between HgCdTe and AlGaAs Heterostructure Quantum Well laser Systems*, University of Baghdad, (2015).

[14] S. Khanna and S. Nivedita, "Recombination of Charge Carriers in p-n Junction Semiconductor", *IJIRT* 1(6) (2014): 1659-1662.

[15] B. A. Ikyo, "electron hole and photon recombination processes in quantum well semiconductor lasers", *American Journal of optics and photonics* 3(5) (2015): 80-84.

[16] B. Gonul and M. Oduncuoglu, "A theoretical comparison of the pressure dependence of the threshold current of phosphorus-aluminium- and nitrogen-based 1.3 µm lasers", *Semiconductor science and technology* 19(1) (2003): 23-32.

[17] H. Zhao, G. Liu, J. Zhang, R. A. Arif and N. Tansu, "current injection efficiency induced efficiency droop in InGaN quantum well light-emitting diodes", *Solid State electronics* 54(10) (2010): 1119-1124.

[18] C. Hamaguchi, *Basic Semiconductor Physics*, Berlin: Springer, (2001).

[19] W. J. Fan, M. F. Li, T. C. Chong and J. B. Xia, "Valence hole subbands and optical gain spectra of $GaN/Ga_{1-x}Al_xN$ strained quantum wells", *Journal of applied physics* 80(6) (1996): 3471-3478.

[20] T. Numai, *Laser Diodes and Their Applications to Communications and Information Processing*, John Wiley & Sons, (2011).

[21] H. A. Makarimi, *Threshold current temperature dependence of indium phosphide quantum dot lasers*. Diss. Cardiff University, (2014).

[22] A. Joullie, P. Christol, A. N. Baranov and A. Vicet, "Mid-infrared 2-5 µm Heterojunction Laser Diodes", *Solid State Mid-infrared Laser Sources Topics Appl. Phys*. 89 (2003): 1-61.

[23] R. R.Hasan and R. Basak, "Characteristics of a Designed 1550 nm AlGaInAs/InP MQW VCSEL", *International Journal of Multidisciplinary Sciences and Engineering* 4(1) (2013).